Real-Time Simulation of Electric Vehicle Battery Charging Systems

Li Bao
Department of Electrical Engineering
University of South Florida
Tampa, FL, 33620, US
libao@mail.usf.edu

Lingling Fan
Department of Electrical Engineering
University of South Florida
Tampa, FL, 33620, US
linglingfan@usf.edu

Zhixin Miao
Department of Electrical Engineering
University of South Florida
Tampa, FL, 33620, US
zmiao@usf.edu

***Abstract*—The sale of electric vehicles (EVs) is rapidly increasing around the world due to EVs' efficiency and energy security. Charging systems play a vital role in electric vehicle. Charging systems can be categorized into three levels according to Society of Automatic Engineers (SAE). This paper presents the topologies of three types of charging systems. The charging systems are simulated in RT-Lab real-time simulator. The input ac for Level 1 and Level 2 charging systems is single-phase. The charging system consists of a diode bridge rectifier, a power factor correction (PFC) boost circuit, a DC/AC converter, an LLC resonant converter, a high frequency transformer, and a diode bridge rectifier. Constant current/constant voltage (CC/CV) control is employed for the DC/AC converter. The Level 3 charging system uses a three-phase source as input and its bi-directional converter is equipped with reactive power and DC bus voltage control. Three testbeds are setup to simulate the three types of charging systems with different charing power levels. A 10 kW-battery will be charged. Simulation results demonstrate the expected charging performance of the charging systems.**

***Index Terms*—Electric vehicle battery charging, CC/CV control, RT-Lab simulation**

I. Introduction

Governments and organizations around the world are taking various efforts to address green house gas emissions associated with fossil fuel burning. Transportation is one among these efforts. According to the Department of Energy, internal combustion engines (ICE) account for 15% of total fossil fuel consumption. However, ICEs show low efficiency and emit carbon dioxide, nitrogen oxides and other poisonous gases. Plug-in electric vehicle (PEV) and electric vehicle (EV) are promising approaches to achieve these goals. They use electricity as the major energy source and are able to reduce green house gas emission and fossil fuel usage significantly [1], [2]. Compared with ICE, PEV and EV offer much higher efficiency and more cost benefits [3]. For example, EVs spend 2 cents per mile while ICE vehicles spend 12 cents per mile [4]. Thanks to these benefits, PEV and EV sale hit a record in 2016, with 750,000 sold worldwide and 40% growth rate compared with the previous year according to the Global EV Outlook 2017 [5]. In this paper, both EVs and PEVs are referred as EVs.

Battery plays a vital role and consists of one-third cost in an EV. The battery capacity range usually is 5 kWh to 50 kWh. An EV can be charged at home, workplace or a dedicated station. A charger is necessary because the grid is alternative current (AC)-based while a battery requires direct current (DC) voltage. Thus the charger consists of AC/DC converters.

According to SAE's EV charging standard, there are three levels of charging based on power ratings. The charging levels are summarized in Table I [6]. Level 1 charging is slow charging and uses convenience household outlet of 120 V. The estimated charging time is about 12 hours. Level 2 is the primary charging method for private and public. The charging voltage is 240 V AC and the charging current is up to 80 A [7]. Level 3 is fast charging with over 20 kW power level.

TABLE I
Charging levels summarization

Charging Level	Supply Voltage	Charging Current	Rating Power
Level 1	120 V, single-phase	up to 16 A	up to 1.92 kW
Level 2	240 V, single-phase	up to 60 A	up to 14.4 kW
Level 3	Not finalized, 3-phase	Not finalized	over 20 kW

In this paper, the three types charging systems are designed and simulated in RT-Lab. This paper is organized as follows. The single-phase chargers for Level 1 and Level 2 are presented in Section II. Topology and controls are analyzed in this section. Section III presents a three-phase charger suitable for Level 3 charging. Section IV provides RT-Lab based simulation results. Section V concludes the paper.

II. Level 1 and Level 2 charging systems

A single-phase AC input is used for both Level 1 and Level 2 charging. The charging circuit includes a diode rectifier, followed by a PFC boost DC/DC converter, and a dual bridge DC/DC converter. The dual bridge DC/DC converter consists of a full bridge DC/AC converter, an LLC resonant converter, a high frequency transformer, and a diode-bridge rectifier. The circuit is shown in Fig. 1. Dual bridge DC/DC converters have been adopted due to its capability of avoiding deadtime and reducing current ripples [8]. A similar topology has been presented in [9]. In this paper, we also adopt LLC resonant converter in the dual bridge DC/DC converter. The LLC resonant converter ensures a near sinusoidal waveform [10].

The PFC boost circuit aims to keep a unity power factor for the power consumption and regulate the output voltage

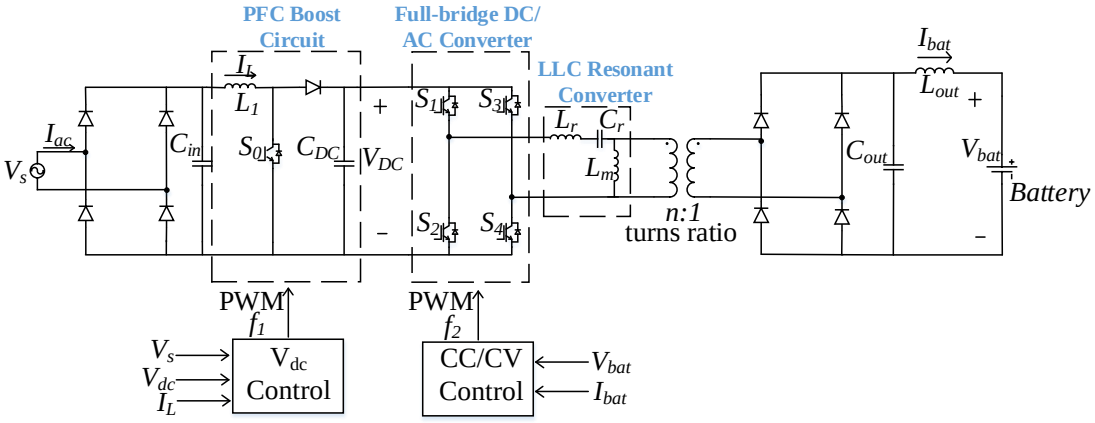

Fig. 1. Topology of a Level 1 or Level 2 charging system.

V_{DC}. CC/CV battery charging control algorithm is implemented through the DC/AC converter control. The topology and control strategies will be analyzed as follows.

A. Battery model

The battery system is a central element of an EV. This element releases storage energy to supply a working EV. In order to ensure an efficient management of battery state-of-charge (SOC) and predict both runtime and I-V performance, a detailed simulation model is needed. The battery model presented in MATLAB/SimPowerSystems library is adopted for this project.

According to [11], there are three categories of battery models: experimental, electrochemical, and electric circuit-based model. The electrochemical model is complex and time-consuming due to its time-varying partial differential equations [12]. The experimental and electrochemical models need high computation ability to solve partial differential equations. The electric circuit model is the most intuitive for simulation. In this paper, a lithium-ion (Li-ion) battery is used and its electric circuit model is adopted for simulation. The model is shown in Fig. 2 [13].

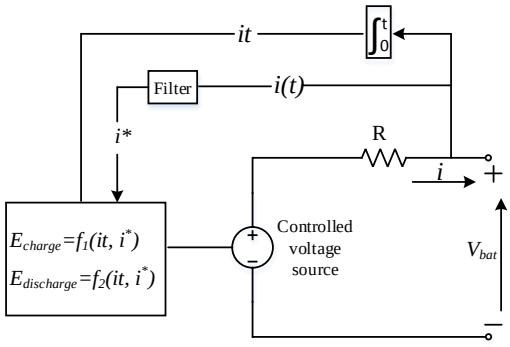

Fig. 2. Li-ion battery non-linear model.

The controlled voltage source is connected in series with a resistor that represents the internal resistance of the battery. The voltage is based on two empirical mathematical expressions shown in Fig. 2, where $f_1(it, i^*)$ is for charging and $f_2(it, i^*)$ for discharging. $f_1(it, i^*)$ and $f_2(it, i^*)$ are defined as follows.

$$f_1(it, i^*) = E_0 - K\frac{Q}{Q - it} \cdot i^* - K\frac{Q}{Q - it} \cdot it + Ae^{-B \cdot it}$$

$$f_2(it, i^*) = E_0 - K\frac{Q}{it - 0.1 \cdot Q} \cdot i^* - K\frac{Q}{Q - it} \cdot it + Ae^{-B \cdot it}$$

where E_0 is constant voltage, K is polarization constant in $\text{Ah}^{-}1$ or in Ω, it is extracted capacity, i^* is filtered current with only slow dynamics and i is battery current, A is exponential zone amplitude, B is the exponential capacity, and Q is the maximum capacity.

In this paper, the parameters are from MATLAB/SimPowerSystems and are shown in TABLE II.

TABLE II
BATTERY PARAMETERS

Nominal Voltage	250 V
Rated capacity	40 Ah
Constant voltage E_0	325 V
Polarization resistance K	0.042 Ω or Ah^{-1}
Maximum capacity Q	45.5 Ah
Internal resistance R	0.0625 Ω
Exponential zone amplitude A	266.7 V
Exponential zone capacity B	11.2 Ah^{-1}

B. PFC boost circuit

The Level 1 and Level 2 charging can take place at home, so the charger should be able to deliver the single-phase residential source (120 V or 240 V) to the battery pack with 200 V to 400 V [14]. The charger should also be capable to allow input current up to 60 A when maximum output occurs.

Since the battery voltage is up to 400 V, we can choose this value as the PFC boost circuit output. According to the Table I, the maximum rating power is 14.4 kW. Hence, the DC current is $\frac{14.4\text{ kW}}{400\text{ V}} = 36$ A.

Assuming unity power factor, the single-phase ac circuit will have the following form of instantaneous power.

$$p(t) = P + P\cos(2\omega t) \tag{1}$$

where ω is 377 rad/s and P is the active power.

The second harmonic ripple component is expected to be absorbed by the capacitor C_{DC}. Further, the DC voltage is assumed to be constant at V_{DC}. The DC current can then be found as $I_{\mathrm{out}} = \frac{P}{V_{\mathrm{DC}}}$. The current through the capacitor should be a second harmonic ripple as:

$$i_c(t) = \frac{P\cos(2\omega t)}{V_{\mathrm{DC}}} = I_{\mathrm{out}}\cos(2\omega t). \tag{2}$$

The related second harmonic component of the capacitor voltage can be found by integrating the capacitor current.

$$v_{c2}(t) = \frac{1}{C_{\mathrm{DC}}}\int i_c(t)dt = \frac{I_{\mathrm{out}}}{2\omega C_{\mathrm{DC}}}\sin(2\omega t). \tag{3}$$

The peak to peak voltage ripple can then be expressed as follows:

$$\Delta V_C = \frac{I_{\mathrm{out}}}{2\pi f C_{\mathrm{DC}}} \tag{4}$$

If the peak-to-peak voltage ripple is less than 10 V, and current is 36 A, the capacitor is chosen as 9.5 mF.

The Level 1 charging voltage is 120 V (RMS), and the output DC voltage is designed to be 400 V.

Then the duty ratio of the boost converter is $D = \frac{V_{\mathrm{out}}-V_{\mathrm{in}}}{V_{\mathrm{out}}} = 0.7$, where V_{out} is the output DC voltage at 400 V. V_{in} is the input DC voltage. For a 120 V AC input which is then rectified, the DC component of the rectified voltage can be found from integration and is $\frac{2}{\pi}V_{\mathrm{peak}}$, approximately at 120 V.

The relationship between the current and voltage of the inductor is as follows.

$$V_L = L\frac{di}{dt} \Rightarrow V_{\mathrm{out}} - V_{\mathrm{in}} = L\frac{\Delta i_L}{DT} \tag{5}$$

where T is the switching time as $5 \times 10^{-4}s$.

If 1 A ripple is allowed, then the inductor can be chosen as 98 mH.

The PFC controller aims to achieve unity power factor by ensuring the input AC current and the input AC voltage have the same phase shift. The charging system is expected to behave similar as a pure resistor. Thus, in this case, the rectified current should be following the rectified voltage $|v_s|$.

Fig. 3 illustrates the impact of PFC control. The current and voltage in the system with PFC control almost have the same phase angles. Without PFC, harmonics and phase shift are shown in the current waveform.

The PFC controller has a cascaded control loop: inner loop is for inductor current control and outer loop is for V_{DC} control. Fig. 4 shows a PFC controller block. The DC bus voltage V_{DC} of the boost circuit is compared with a fixed reference voltage. The error goes to a PI controller and then is multiplied with the rectified voltage to generate a reference inductor current. The reference current is proportional to the rectified voltage. The inner loop regulates the current to follow the reference current. The error between the reference current and the measured current is the input to a PI controller. The output is the duty cycle of the PFC boost converter. This signal is compared with a triangle waveform to generate pulse width modulation (PWM)-based switching sequences for the switches.

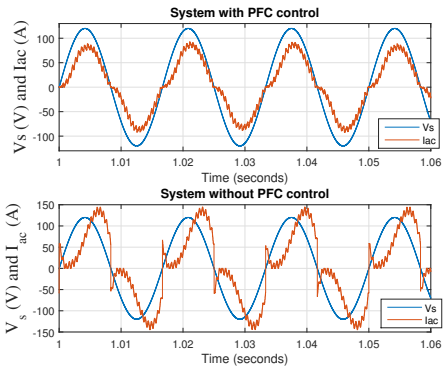

Fig. 3. Comparison of I_{ac} and V_{s} for PFC control and without PFC control.

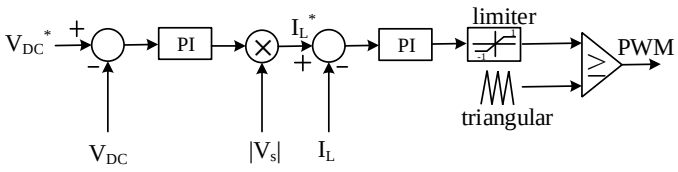

Fig. 4. PFC boost circuit control block [15].

C. CC/CV charging algorithm

There are several charging methods that can be applied in EV battery charging. The three basic methods are constant-current (CC), constant-voltage (CV) and taper-current (TC) charging [16]. The CC method charges a battery using a constant charging current while voltage varies. When the voltage reaches a preset value, the charging process will stop. However, the charging current level needs to be considered carefully because low current is not suitable for fast charging while high current may cause excessive damage. The CV method limits the voltage to a specific level by varying current. The charging stops until current drops to almost zero. The TC method charging a battery with a decreasing current while the voltage is rising. The method rarely used since batteries have different characteristics in real application.

CC/CV charging is combination of CC and CV, and intends to enhance the reliability and efficiency. The CC method is usually used in the initial stage of charging to avoid over current. The CV method is used following the initial stage. Fig. 5 shows a simple illustration of CC/CV charging.

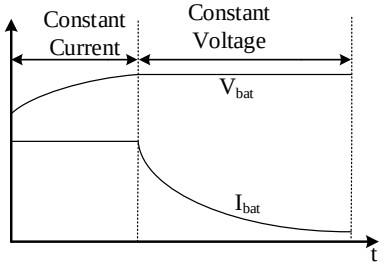

Fig. 5. Illustration of CC/CV charging.

Firstly the battery charging is operated at CC mode, where charging current is kept as constant and charging voltage is increasing. The control will change to CV mode when voltage reaches a preset value. When the current drops to cut-off value, the charging will stop. Usually the CV mode takes same or longer time than CC.

The control implementation is shown in Fig. 6 [17]. The CC/CV selector compares the battery voltage with a preset value to switch charging mode.

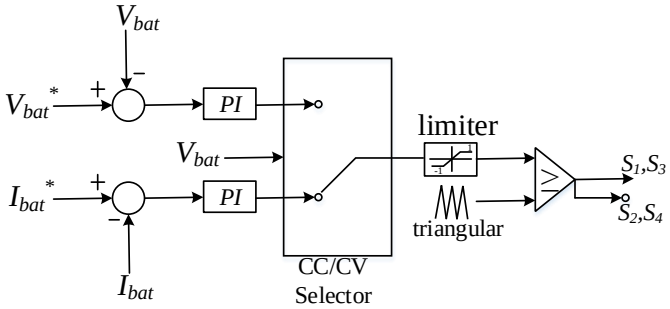

Fig. 6. CC/CV charging structure, when battery voltage reaches a preset value, the selector will turn to voltage PI controller.

The parameters of Level 1 and Level 2 charging systems are listed in Table. III.

TABLE III
PARAMETERS OF LEVEL 1 AND LEVEL 2 CHARGING SYSTEMS

Parameter	Value	Parameter	Value
C_{in}	20 mF	L_1	98 mH
C_{DC}	9.5 mF	L_{r}	2.8 mH
C_{r}	30 μH	L_{m}	20 mH
C_{out}	1 mF	L_{out}	10 mH
f_1	2000 Hz	f_2	500 Hz
V_{dc}^*	300 V	$V_{\text{s\_level1}}$	120 V
$V_{\text{s\_level2}}$	240 V	n	1
PFC circuit inner loop control		$0.001 + \frac{0.1}{s}$	
PFC circuit outer loop control		$0.003 + \frac{0.3}{s}$	
CC/CV current control		$0.0015 + \frac{0.15}{s}$	
CC/CV voltage control		$20 + \frac{2}{s}$	

III. LEVEL 3 CHARGING CIRCUIT TOPOLOGY

According to Table I, a Level 3 charging system has a three-phase source as input. Thus, the system includes a three-phase AC/DC converter. In this paper, we adopt a bi-directional converter based on IGBT switches. Considering vehicle to grid (V2G) services, we apply V_{DC}/Q control. The V_{DC}/Q control can regulate the DC bus voltage and the reactive power from grid. The topology of Level 3 charger is shown in Fig. 7.

The V_{DC}/Q control structure is shown in Fig. 8. The controller has two inputs: reactive power measurement and DC bus voltage measurement. Two PI controllers are used to make sure the measurements track their reference values. The outputs from the PI controllers are dq-axis current orders. This dq-reference frame is aligned with the input voltage space vector. Angle of the input voltage space vector (θ) is obtained through a PLL. This angle is used for abc–dq and dq–abc conversion.

The dq-axis current orders are converted to abc three-phase current orders, notated in Fig. 8 as $\mathbf{i}_{\text{grid}}^*$. Three proportional resonant (PR) controllers are then used to guarantee that the abc current measurements track the grid current orders. The outputs of the PR controllers are abc-frame converter voltages. After scaling, these signals will be used to generate PWM signals. Grid voltage v_a, v_b and v_c are transformed to the dq frame by using Park transformation and θ from phase-locked-loop (PLL) [18].

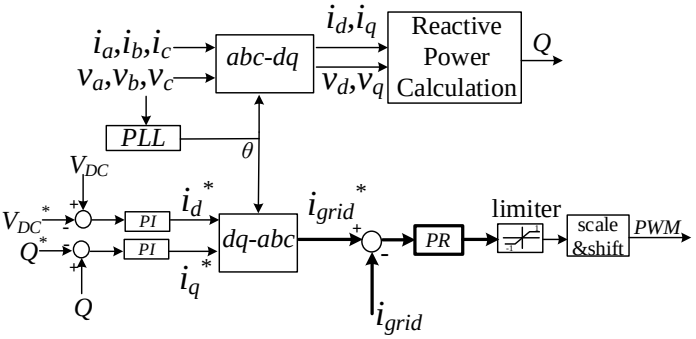

Fig. 8. V_{DC}/Q control method applied to the three-phase rectifier.

The transformed voltage and current are used to calculate three-phase reactive power as shown follows:

$$Q = \frac{3}{2}(v_q i_d - v_d i_q). \tag{6}$$

The block diagram of the PR controller has been illustrated in Fig. 9.

A second-order PLL is modeled in this project. Its control block is shown in Fig. 10 [19]. The inputs of PLL are three-phase grid voltages v_a, v_b, and v_c. They are converted into dq-axis voltages based on the angle θ obtained from PLL. PLL works to synchronize the charging system to the grid.

In RT-Lab, all PI and PR controllers are based on real values. Discrete controllers are implemented for fixed time step simulation. The diagram block of a PI controller is shown in Fig. 11.

The parameters of the Level 3 charging system are given in Table IV.

TABLE IV
PARAMETERS OF LEVEL 3 CHARGING SYSTEM

R_{grid}	0.003 Ω
L_{grid}	3 mH
V_{grid}	150 V 3-phase
PLL	$k_p = 180$, $k_i = 3200$
V_{DC}^*	330 V
V_{DC} PI controller	$0.1 + \frac{10}{s}$
Reactive power PI controller	$0.1 + \frac{1}{s}$
PR controller	$k_p = 500$, $k_r = 50$, $\omega = 2\pi \times 60$

IV. SIMULATION RESULTS

The simulation of the three testbeds with proposed parameters and control strategies are conducted in RT-Lab environment for 1500 seconds (25 minutes). The battery has a

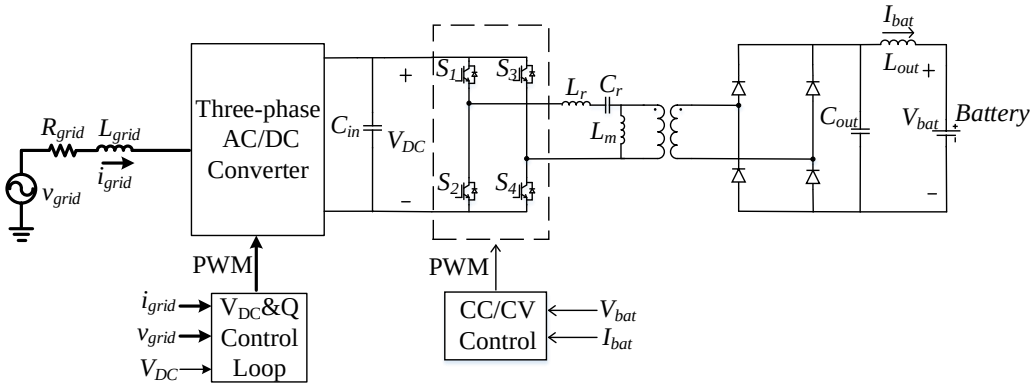

Fig. 7. Topology of level-3 charging system, bold elements mean three-phase form.

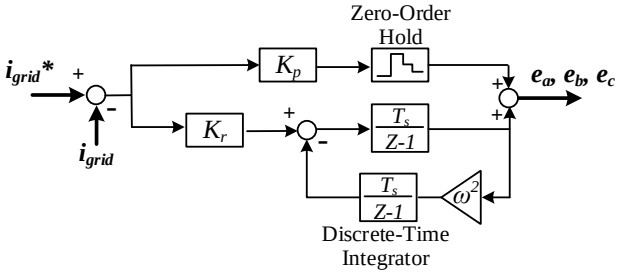

Fig. 9. Structure of PR controller. e_a, e_b and e_c notate the voltages from the bi-directional converter.

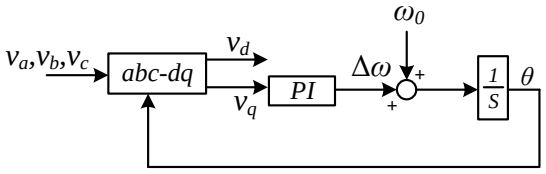

Fig. 10. Block diagram of a PLL.

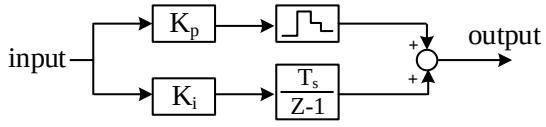

Fig. 11. Block diagram of a discrete PI controller.

power rating of 10 kW and its capacity is 40 Ah. The overall simulation results are shown in Figs. 12-13. The results include battery voltage, current and SOC. The CC/CV charging control is realized in the simulation.

For Level 1, charging starts with 5 A and voltage increases from 265.5 V. When the voltage reaches the preset value 266.5 V, charging turns to CV mode. Then the voltage keeps as 266.5 V and current starts to decreases. The DC bus voltage V_{DC} in controlled by PFC boost controller and keeps as 300 V. Charging power decreases when charging changes to CV mode. For Level 2 and Level 3, their charging current are 40 A and 80 A, preset voltage are 273.5 V and 280 V, respectively. Fig. 13 provides the SOC comparison of three level charging. Note that in 25 minutes, Level 3 charging makes the SOC increase from 20% to 85%, Level 2 charging increases the SOC from 20% to 60%, while Level 1 charging increases SOC less than 5%.

The simulation results are summarized in Table V. The charging current, voltage and rating power are corresponded to the SAE standard. Estimated fully charging time indicates the time that charge battery from 0% SOC to 100%.

TABLE V
SIMULATION ANALYSIS

	Level 1	Level 2	Level 3
Initial SOC	20%	20%	20%
Duration time	1500s	1500s	1500s
DC bus voltage	300 V	300 V	330 V
Charging power	1.33 kW	10.94 kW	22.48 kW
Constant current	5 A	40 A	80 A
Constant voltage	266.5 V	273.5 V	281 V
End SOC	24.3%	58.4%	84.3%
Estimated fully charging time	10 hours	1.1 hour	40 mins

V. CONCLUSION

This paper has presneted the topologies and control strategies of three types of EV charging systems for Level 1, Level 2, and Level 3. Three testbeds consisting of power electronic converter circuits and controls are built in RT-Lab environment. The Level 1 and Level 2 charging systems use sing-phase AC source and consist of a diode-bridge rectifier, a PFC boost circuit, and a dual-bridge DC/DC converter. The Level 3 charging system uses three-phase AC source and consists of a bi-directional DC/AC converter and a dual-bridge DC/DC converter. V_{DC}/Q control is adopted for the bi-directional DC/AC converter. CC/CV battery charging control is implemented in the DC/DC dual bridge converter. RT-Lab simulation results show expected charging processes.

REFERENCES

[1] M. Yilmaz and P. T. Krein, "Review of battery charger topologies, charging power levels, and infrastructure for plug-in electric and hybrid vehicles," *IEEE Transactions on Power Electronics*, vol. 28, no. 5, pp. 2151–2169, May 2013.

[2] ——, "Review of the impact of vehicle-to-grid technologies on distribution systems and utility interfaces," *IEEE Transactions on Power Electronics*, vol. 28, no. 12, pp. 5673–5689, Dec 2013.

[3] S. G. Wirasingha and A. Emadi, "Pihef: Plug-in hybrid electric factor," in *2009 IEEE Vehicle Power and Propulsion Conference*, Sept 2009, pp. 661–668.

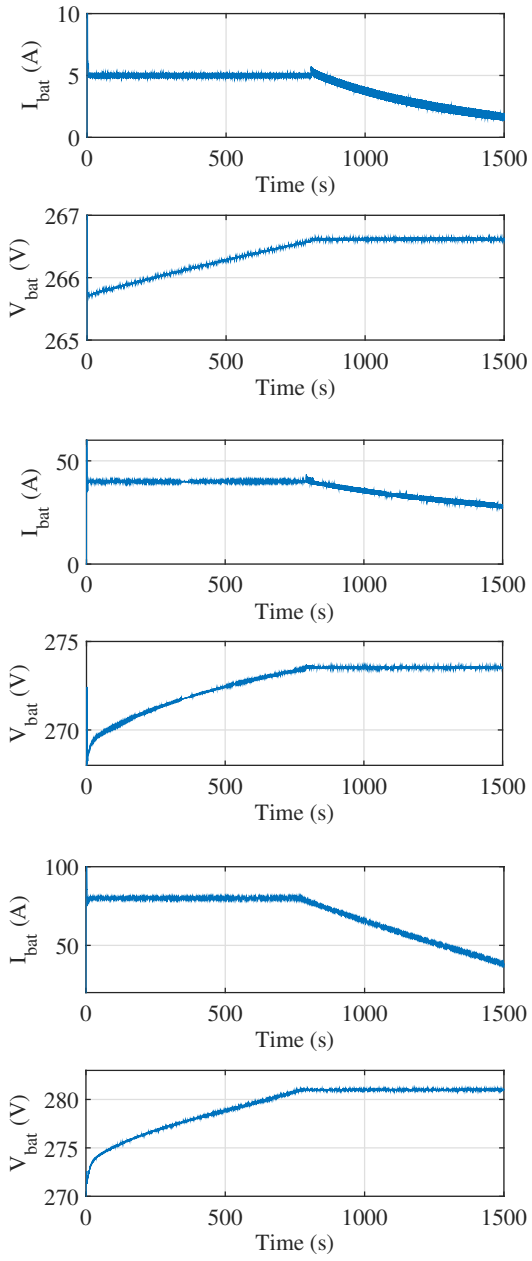

Fig. 12. Three charging processes. From upper to bottom: Level 1, Level 2, Level 3.

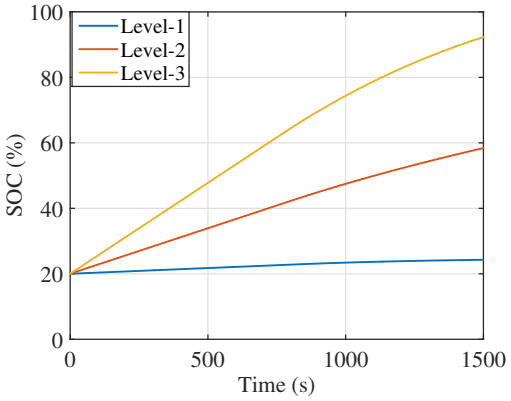

Fig. 13. SOC comparison of three level charging.

[4] S. F. Tie and C. W. Tan, "A review of energy sources and energy management system in electric vehicles," *Renewable and Sustainable Energy Reviews*, vol. 20, pp. 82 – 102, 2013. [Online]. Available: http://www.sciencedirect.com/science/article/pii/S1364032112006910

[5] I. E. Agency, "Global ev outlook 2017," June 2017. [Online]. Available: https://www.iea.org/publications/freepublications/publication/GlobalEVOutlook2017.pdf

[6] J. Y. Yong, V. K. Ramachandaramurthy, K. M. Tan, and N. Mithulananthan, "A review on the state-of-the-art technologies of electric vehicle, its impacts and prospects," *Renewable and Sustainable Energy Reviews*, vol. 49, pp. 365 – 385, 2015. [Online]. Available: http://www.sciencedirect.com/science/article/pii/S1364032115004001

[7] D. Aggeler, F. Canales, H. Zelaya, D. L. Parra, A. Coccia, N. Butcher, and O. Apeldoorn, "Ultra-fast dc-charge infrastructures for ev-mobility and future smart grids," in *2010 IEEE PES Innovative Smart Grid Technologies Conference Europe (ISGT Europe)*, Oct 2010, pp. 1–8.

[8] W. Song and B. Lehman, "Dual-bridge dc-dc converter: a new topology characterized with no deadtime operation," *IEEE Transactions on Power Electronics*, vol. 19, no. 1, pp. 94–103, Jan 2004.

[9] J.-S. Kim, G.-Y. Choe, H.-M. Jung, B.-K. Lee, Y.-J. Cho, and K.-B. Han, "Design and implementation of a high-efficiency on- board battery charger for electric vehicles with frequency control strategy," in *2010 IEEE Vehicle Power and Propulsion Conference*, Sept 2010, pp. 1–6.

[10] J. Wu, Y. Li, X. Sun, and F. Liu, "A new dual-bridge series resonant dc/dc converter with dual tank," *IEEE Transactions on Power Electronics*, vol. 33, no. 5, pp. 3884–3897, May 2018.

[11] D. W. Dees, V. S. Battaglia, and A. Blanger, "Electrochemical modeling of lithium polymer batteries," *Journal of Power Sources*, vol. 110, no. 2, pp. 310 – 320, 2002. [Online]. Available: http://www.sciencedirect.com/science/article/pii/S0378775302001933

[12] L. Song and J. W. Evans, "Electrochemical-thermal model of lithium polymer batteries," *Journal of the Electrochemical Society*, vol. 147, no. 6, pp. 2086–2095, 2000.

[13] O. Tremblay and L.-A. Dessaint, "Experimental validation of a battery dynamic model for ev applications," *World Electric Vehicle Journal*, vol. 3, no. 1, pp. 1–10, 2009.

[14] P. T. Krein, *Elements of power electronics*. Oxford University Press New York, 1998, vol. 126.

[15] C. Zhou, R. B. Ridley, and F. C. Lee, "Design and analysis of a hysteretic boost power factor correction circuit," in *21st Annual IEEE Conference on Power Electronics Specialists*, 1990, pp. 800–807.

[16] C. H. Dharmakeerthi, N. Mithulananthan, and T. K. Saha, "Modeling and planning of ev fast charging station in power grid," in *2012 IEEE Power and Energy Society General Meeting*, July 2012, pp. 1–8.

[17] A. Tazay and Z. Miao, "Control of a three-phase hybrid converter for a pv charging station," *IEEE Transactions on Energy Conversion*, 2018.

[18] A. R. Bergen, *Power systems analysis*. Pearson Education India, 2009.

[19] L. Fan, *Control and Dynamics in Power Systems and Microgrids*. CRC Press, 2017.